# Model Reference Adaptive Control for Squirrel-Cage Induction Generator-Based Wind Energy Conversion Systems

Ismael. A. de Azevedo, Luciano. S. Barros, Caio. D. Cunha

***Abstract*—For maximum power point tracking of squirrel-cage induction generator-based wind energy conversion systems, control strategies may face some difficulties such as: unmodeled dynamics, variable reference and disturbances. Adaptive controllers may offer good reliability and robustness against these issues, for these reasons, in this work a model reference adaptive controller is applied. In order to test the proposed controller, simulation comparison in Matlab/Simulink with the traditional PI control is carried out. The topology used is a generator connected to the grid by a full power back-to-back converter. Flux and torque are controlled by a vectorial strategy. The results suggest that the adaptive control is better than the PI in a parametric uncertainty scenery and can be applied in wind energy conversion systems.**

***Keywords*—Model Reference Adaptive Controller, Adaptive Control, Squirrel Cage Induction Generator, Wind Energy.**

## I. Introduction

THE last two decades has proven that wind energy conversion systems (WECS) are not only a promise of a renewable energy source for the future, but it is a source of clean energy of today. The numbers of the annual installed capacity by region suggest a tendency of continuous growing [1].

There are lots of topologies of WECS with different types of generators: permanent magnet synchronous generator (PMSG), double fed induction generator (DFIG) and squirrel cage induction generator (SCIG). DFIG is popular due to its low cost converter, high energy yields and compact size [2]. PMSG is being used due to its flexibility in velocity control, reduced weight and low maintenance [3]. SCIG is the cheapest and it has good reliability and robustness [4].

In [4] it showed a control strategy based on an indirect field oriented control (IFOC) scheme, using a SCIG with the traditional PI and a back-to-back converter. The results proved a good transient response in the decoupled real and reactive powers. In [5] it showed a SCIG connected to the grid through a full power converter driven by vector control. The control scheme enables the system to control the stator-side converter without flux sensor inside the machine. The control strategy was satisfactory. The application of direct torque control (DTC), presented in [6], with space vector modulation of two or three levels inverter, produced improved transient responses and reference tracking performance of the voltage in the generator and grid sides as well the DC link. For simplicity and good performance, this paper presents a DTC strategy and a two levels full power inverter back-to-back scheme.

Adaptive control can offer good properties in WECS such as: good performance against unmodeled dynamics, insensitivity to parameter variations, external disturbance rejection and fast dynamic response [7]. These kinds of issues were dealt in many studies [8], [9], [10], [11], [12], [13]. This work seeks to solve the problem of uncertainty parameters in an other way.

This paper presents a simulation which uses a model reference adaptive controller (MRAC) [7] applied in a WECS based on a SCIG. The aerodynamic model and the control of the grid are similar to [14], [15]. The MRAC model is similar to [16].

It covers six sections. The second one describes the model of the machine. The third presents the machine-side and the grid-side controls and the PWM model. The fourth explains how the MRAC was applied. The fifth section discusses the results, followed by the conclusion in the sixth section.

## II. Model

### A. Machine Model

The squirrel cage induction generator can be described by three windings in the stator and three in the rotor. There are some assumptions that are made to simplify the model: the windings are equals and shifted by 120 degrees among them, the air gap is considered constant, the magnetic circuit is ideal and the flux density distribution in the gap is sinusoidal. The fluxes, voltages and the electromagnetic torque are given by:

$$\phi_{s123} = \overline{L}_{ss} i_{s123} + \overline{L}_{sr} i_{r123}; \tag{1}$$

$$\phi_{r123} = \overline{L}_{rs} i_{s123} + \overline{L}_{rr} i_{r123}; \tag{2}$$

$$v_{s123} = R_s i_{s123} + \frac{d\phi_{s123}}{dt}; \tag{3}$$

$$v_{r123} = R_r i_{r123} + \frac{d\phi_{r123}}{dt}; \tag{4}$$

$$T_e = P i_{s123}^T \frac{d\overline{L}_{sr}}{d\theta} i_{r123}. \tag{5}$$

Where:

I. A. de Azevedo (ismaelaz@hotmail.com), L. S. Barros (lsalesbarros@dee.ufrn.br) and C. D. Cunha (dorneles@ufrnet.br) are with the Federal University of Rio Grande do Norte (UFRN), Natal, Brazil.

Paper submitted to the International Conference on Power Systems Transients (IPST2019) in Perpignan, France June 17-20, 2019.

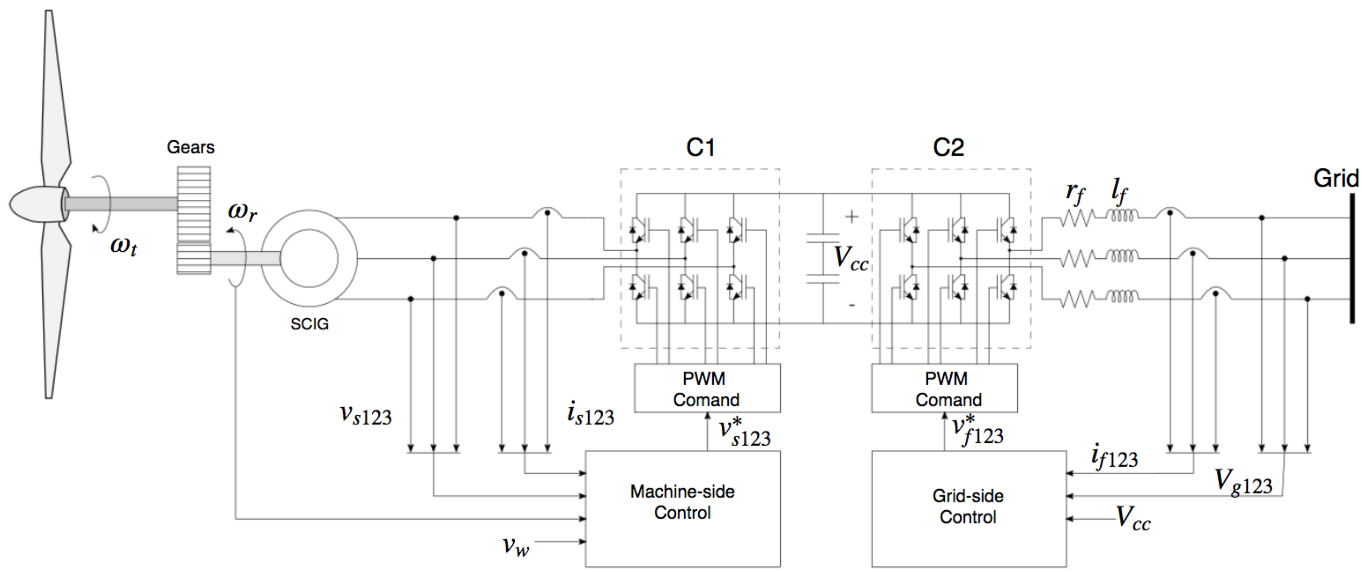


Fig. 1. Wind Energy Conversion Systems

$$i_{s123} = \begin{bmatrix} i_{s1} \\ i_{s2} \\ i_{s3} \end{bmatrix} \quad v_{s123} = \begin{bmatrix} v_{s1} \\ v_{s2} \\ v_{s3} \end{bmatrix} \quad \phi_{s123} = \begin{bmatrix} \phi_{s1} \\ \phi_{s2} \\ \phi_{s3} \end{bmatrix}$$

$$i_{r123} = \begin{bmatrix} i_{r1} \\ i_{r2} \\ i_{r3} \end{bmatrix} \quad v_{r123} = \begin{bmatrix} v_{r1} \\ v_{r2} \\ v_{r3} \end{bmatrix} \quad \phi_{r123} = \begin{bmatrix} \phi_{r1} \\ \phi_{r2} \\ \phi_{r3} \end{bmatrix}$$

$$L_{ss} = \begin{bmatrix} L_s & M_s & M_s \\ M_s & L_s & M_s \\ M_s & M_s & L_s \end{bmatrix} \quad L_{rr} = \begin{bmatrix} L_r & M_r & M_r \\ M_r & L_r & M_r \\ M_r & M_r & L_r \end{bmatrix}$$

$$\text{K}= \begin{bmatrix} \cos(\theta) & \cos(\theta+2\pi/3) & \cos(\theta+4\pi/3) \\ \cos(\theta+4\pi/3) & \cos(\theta) & \cos(\theta+2\pi/3) \\ \cos(\theta+2\pi/3) & \cos(\theta+4\pi/3) & \cos(\theta) \end{bmatrix}$$

$$L_{rs}(\theta) = M_{sr}\text{K}$$

$$L_{rs}(\theta) = L_{sr}(\theta)'$$

$$\frac{d\overline{L}_{sr}}{d\theta} = M_{sr}\ \frac{dK}{d\theta}$$

$i_{s123}$, stator's current in the phases 1,2 and 3 (A);
$i_{r123}$, rotor's current in the phases 1,2 and 3 (A);
$\phi_{s123}$, flux of the stator's winding (Wb);
$\phi_{r123}$, flux of the rotor's winding (Wb);
$v_{s123}$, stator's voltage in the phases 1,2 and 3 (V);
$v_{r123}$, rotor's voltage in the phases 1,2 and 3 (V);
$L_s$, self inductance of the stator's winding (H);
$L_r$, self inductance of the rotor's winding (H);
$M_s$, linkage inductance between two stator's winding (H);
$M_r$, linkage inductance between two rotor's winding (H);
$M_{sr}$, linkage inductance between a winding of the stator and a winding of the rotor (H);
$K$, matrix of the angles;
$P$, number of pairs of poles;
$\theta$, electric angular position of the rotor (rad).

## III. Controls

The whole system is shown in the diagram of the Figure 1. It presents the wind turbine, gears, SCIG, converter, filter and the grid.

### A. Machine Side

The machine-side control is responsible to the maximum power point tracking (MPPT). To do this, it has to control the turbine velocity $\omega_t$ in response to the wind variations and keep the optimum power coefficient of the turbine. The speed of the turbine is controlled by the velocity of the rotor $\omega_r$.

Applying the Park Transform to the machine model results in a simplified version to be controlled. The strategy to this paper is a variation of what was presented in [17]. In 0dq, in a generic reference $g$, the equations are:

$$v_s^g = r_s i_s^g + \frac{d\phi_s^g}{dt} + j\omega_g \phi_s^g; \tag{6}$$

$$0 = r_r i_r^g + \frac{d\phi_r^g}{dt} + j(\omega_g - \omega_r)\phi_r^g; \tag{7}$$

$$\phi_s^g = l_s i_s^g + l_m i_r^g; \tag{8}$$

$$\phi_r^g = l_r i_r^g + l_m i_s^g; \tag{9}$$

$$Te = i_s \phi_s \sin(\delta_i - \delta_a) = \frac{l_m}{l_r}\phi_r \sin(\delta_i - \delta_b). \tag{10}$$

The equations for the control are:

$$Te = \frac{P l_m^2 \omega_{ar} \phi_s^2}{r_r l_s^2}; \tag{11}$$

$$\phi_s^{s*} = \phi_s^* e^{j\delta_a^*}; \tag{12}$$

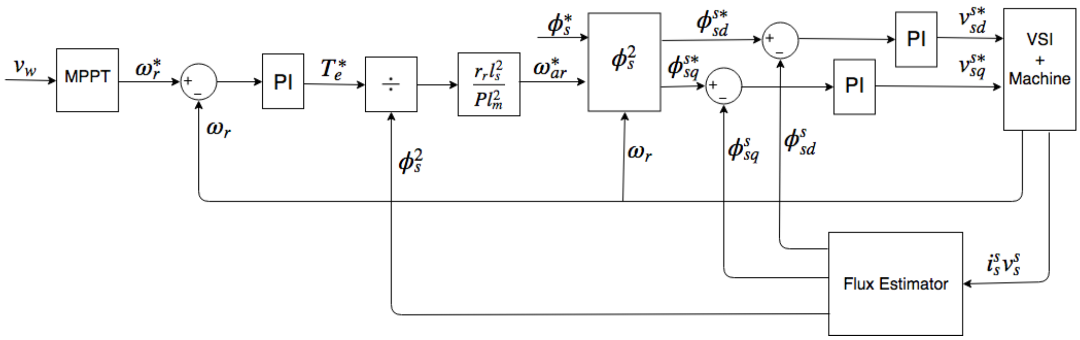


Fig. 2. Machine-side control

$$\delta_a^* = \int_0^t \omega_a r^*(\tau)d\tau + \int_0^t \omega_r(\tau)d\tau; \tag{13}$$

$$v_s^g = \frac{r_s}{\sigma l_s}\phi_s^g + \frac{d\phi_s^g}{dt} - \frac{l_m r_s}{\sigma l_s l_r}\phi_r^g; \tag{14}$$

$$v_{sd}^s = \frac{r_s}{\sigma l_s}\phi_{sd}^s + \frac{d\phi_{sd}^s}{dt} - \frac{l_m r_s}{\sigma l_s l_r}\phi_{rd}^s; \tag{15}$$

$$v_{sq}^s = \frac{r_s}{\sigma l_s}\phi_{sq}^s + \frac{d\phi_{sq}^s}{dt} - \frac{l_m r_s}{\sigma l_s l_r}\phi_{rq}^s. \tag{16}$$

The flux estimator is:

$$\phi_s^s = \int_0^t [v_s^s(\tau) - r_s i_s^s(\tau)]d\tau. \tag{17}$$

The control diagram is shown in the Figure 2.

Where:

$v_s$, stator's voltage vector (V);
$i_s$, stator's current vector (A);
$i_r$, rotor's current vector (A);
$\phi_s$, stator's flux vector (Wb);
$\phi_r$, rotor's flux vector (Wb);
$rs = Rs$, stator's resistance ($\Omega$);
$rr$ = Rr, rotor's resistance ($\Omega$);
$wg$, frequency of a generic referential (rad/s);
$ls = Ls - Ms$, cyclic stator's inductance (H);
$lr = Lr - Mr$, cyclic rotor's inductance (H);
$lm = (3/2)Mrs$, linkage cyclic inductance (H);
$war = wa - wr$, slipe frequency of the stator's flux vector (rad/s);
$\delta_a$, angular position of the stator's flux vector (rad);
$\sigma = 1 - (lm^2)/(lslr)$, dispersion coefficient.

The electromagnetic torque can be controlled by $\omega_{ar}$ since the magnitude of the flux is kept fixed. The flux can be controlled by the current components in $d$ and $q$ stator referential. The control generates the voltage references to the converter C1.

### B. Grid Side

The grid side control is responsible to deliver the power to the grid. The active power control has two parts, the inner is responsible to keep the voltage in the capacitor. The outer controls the current $i_{fd}$. The reactive power of reference controls the current $i_{fq}$. The angle $\theta$ is estimated by the phase-locker loop (PLL). The diagram is shown in the Figure 3.

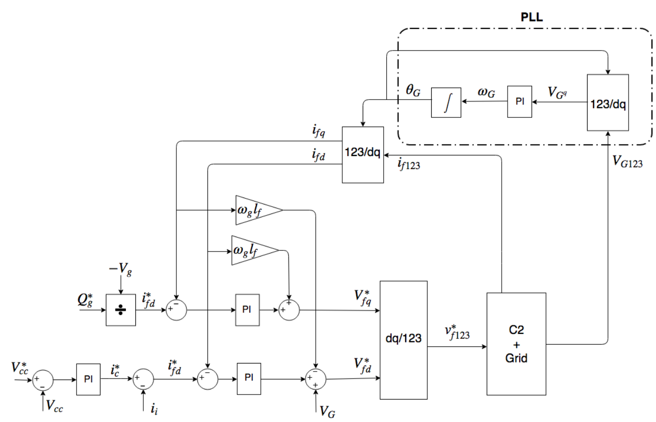


Fig. 3. Grid-side control

Filter model:

$$v_{fd}^G = r_f i_{fd}^G + l_f\frac{di_{fd}^G}{dt} - \omega_G l_f i_{fq}^G + V_G; \tag{18}$$

$$v_{fq}^G = r_f i_{fq}^G + l_f\frac{di_{fq}^G}{dt} - \omega_G l_f i_{fd}^G. \tag{19}$$

Power equations:

$$P_g = V_G i_{fd}^G; \tag{20}$$

$$Q_g = -V_G i_{fq}^G. \tag{21}$$

Dynamic of the capacitor:

$$C\frac{dV_{cc}}{dt} = \frac{P_s - P_f}{V_{cc}}. \tag{22}$$

Where:

$Vf$, voltage vector of the filter applied by the converter (V);
$Vg$, grid's voltage vector (V);
$If$, current vector of the filter (A);
$Wg$, angular frequency of the grid's reference (rad/s);
$Lf$, filter's inductance (H);
$Pg$, active power delivered to the grid (W);
$Qg$, reactive power delivered to the grid (var);
$Vcc$, voltage in the capacitor (V);
$C$, capacitance (F);

$Pi$, power provided by C1 (W);
$Pf$, power provided by C2 (W).

### C. PWM Model

The topology of the converters consists of six insulated gate bipolar transistor (IGBTs), two of them for each branch. The IGBT's of the same phase cannot conduct at the same time.

The Digital-Scalar Pulse Width Modulation (DS-PWM) is used for the switching control and it was presented in [18]. It calculates, for each phase, the interval $\tau$ of time that is needed the switch to conduct.

For each period of PWM the command puts a pole voltage $(va_0, vb_0, vc_0)$ of mean value equals to the sinusoidal reference given by the controller. The pole mean voltage for a phase $j$ is calculated by:

$$\overline{v_{jo}} = v_{ref} = \frac{1}{\tau}[\tau_j \frac{V_{cc}}{2} - (\tau - \tau_j)\frac{V_{cc}}{2}]\frac{1}{\tau} \tag{23}$$

From 23:

$$\tau_j = (\frac{v_{ref}}{V_{cc}} + \frac{1}{2})\tau \tag{24}$$

From this equation, it is possible to determine the interval $\tau$.

## IV. MRAC

### A. MRAC description

The project of a controller is made by a transfer function of a plant. The problem with this kind of approach is that in some cases there are uncertainties, dynamic changes and unknown parameters. The development of an adaptive control is a solution for these problems. The idea is to use the input and the output so that the control can figure out the characteristics of the plant and adjust the controller.

There are two kinds of approaches: direct and indirect. This paper shows the direct way of adjustment. To achieve it, there is the MRAC, which uses an ideal plant in comparison with the real one. The MRAC method control has larger robustness in comparison to fixed parameters controllers. When the output of the plant is equal to the output of the model reference, it is called *matching condition*:

$$\lim_{t\to\infty} e_0(t) = 0. \tag{25}$$

The MRAC strategy requires some assumptions:

- The model reference plant must be Strictly Real Positive (SRP);
- The plant must be controllable and observable;
- $k_p$ and $K_m$ must have the same signal.

For plants with relative degree larger or equal to 2, in [19] it showed that it is necessary to introduce an auxiliary signal, so that the augmented error is ruled by a SRP operator. But, for a first order plant model, the control signal $u$ is given by:

$$u = [\theta_{c1}\theta_{c2}]\begin{bmatrix} y \\ r \end{bmatrix} = \theta^T\omega. \tag{26}$$

$\theta^T$ is the adaptive array and $\omega$ is the regressive array [20]. In order to obtain $\theta^T$, one must integrate the adaptive law, that is given by:

$$\dot{\theta} = -\gamma e_0 \omega, \gamma > 0. \tag{27}$$

In [21] it was shown that the original MRAC is unstable for some unmodeled dynamics and external disturbs. In order to increase robustness in the MRAC, an adaptation law with $\sigma$-modification was proposed [22]. It ensured, at least, the local stability in presence of unmodeled dynamics and external disturbs. Leading to:

$$\dot{\theta} = -\sigma\theta - \gamma e_0 \omega, \sigma > 0. \tag{28}$$

The scheme of this control is shown in the Figure 4:

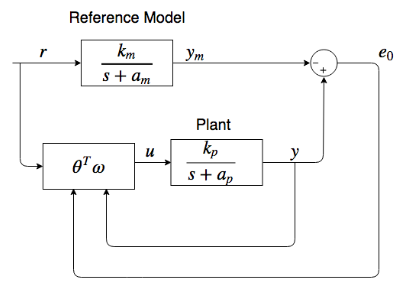


Fig. 4. MRAC scheme

### B. MRAC Application

In order to test the robustness of the MRAC, the parameters of the PI control were calculated by the diofantine equation and then adjusted to achieve the best response possible. The parameters of the MRAC were estimated by try and error method. After these, there was applied a factor of $+1.3$ in the stator's resistance as an uncertainty parameter. A Zero-order hold of $10kHz$ was applied to the signal $y$.

## V. Results

The start-up of the machine is simulated. It is done by a wind turbine, which parameters of are shown in the Table III, coupled to the SCIG.

The first case is presented in the Figure 5. It shows the comparison, with no parametric uncertainty, between the traditional PI control and the proposed MRAC control. The second case is presented in the Figure 6. It shows the results when there is applied a parametric uncertainty at the resistance of the stator.

In the first case, as shown in the Figure 5, when there is no uncertainty, the MRAC offers good response, despite the delayed transient and a fixed delayed in steady state, in the flux $\phi_{sd}^s$ and the flux $\phi_{sq}^s$ due to the fact that $y$ has a low error compared to $y_m$ in both fluxes.The velocity $\omega_r$ followed the reference and the control voltages $v_{s123}^*$ had a smooth, but distorted, response.

### A. Without parametric uncertainty

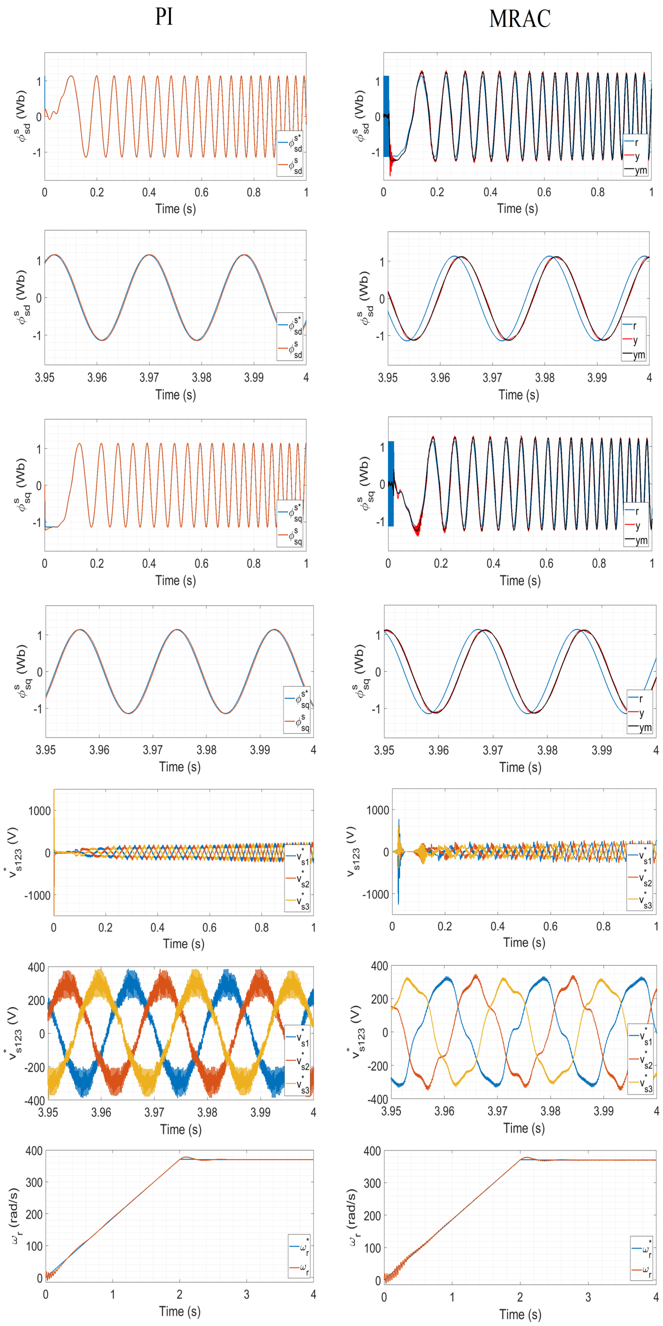


Fig. 5. PI vs MRAC

MRAC presented a good performance, despite the slow response in the transient and the fixed delayed response in steady state. PI presented a good result in the transient and in the steady state.

### B. With parametric uncertainty

In the second case, as shown in the Figure 6, when there is an uncertainty in the resistance, the MRAC offers the same quality of response compared to the first case. On the other hand, despite the PI followed the reference initially, it eventually looses the reference. Due to this, the machine does not accelerate properly and the control voltages $v^*_{s123}$ increased beyond the limit of the converter.

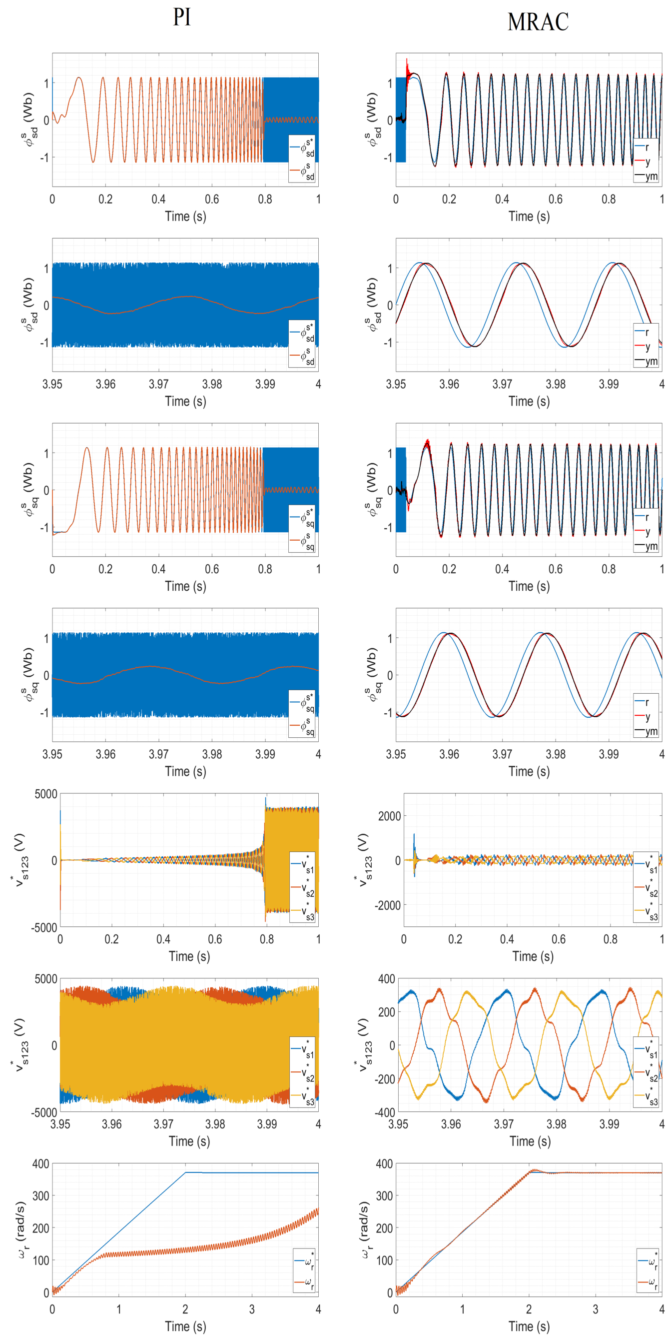


Fig. 6. PI vs MRAC - with uncertainty of 30% in resistance of the stator

## VI. Conclusion

This paper presented a simulation comparison of PI and MRAC applied to a SCIG with a *back-to-back* converter based WECS. As an adaptive controller, MRAC offers reliability and robustness against unmodeled dynamics, variable reference and disturbances.

The results suggest that, if it is needed to project a controller for a plant with uncertainty, the MRAC technique is a good choice even though it has a slow response in the transient and a fixed delayed response in steady state. In order to solve these problems, one may apply a variable state structure [23], but this should increase complexity and result in high frequency control signals.

Moreover, in this paper it shows that MRAC is robust against uncertainty parameters and applicable to wind energy conversion systems, producing good results.

## VII. Appendix

The Table I presents the data used in the machine model. The Table II presents the parameters used in the PI control. The Table III presents the data used in the turbine model. The Table IV presents the parameters used in the MRAC control.

TABLE I
SCIG

| Parameter | Value |
|---|---|
| Voltage | 380/220 ($V$) |
| Power | 3400 ($W$) |
| $R_s and R_r$ | 2.8237 ($\Omega$) |
| $M_s and M_r$ | -0.0994 ($H$) |
| $M_{sr}$ | 0.1989 ($H$) |
| P | 2 |
| $F_m$ | 0.00146 ($N \cdot m \cdot s$) |
| $J_m$ | 0.0133 ($K_g \cdot m^2$) |

TABLE II
PI

| Parameter | $K_p$ | $K_i$ | $K_d$ |
|---|---|---|---|
| $\omega_m$ | 0.1 | 29 | 1.8 |
| $\phi_{sd}$ | 4000 | 380770.4 | 0 |
| $\phi_{sq}$ | 4000 | 380770.4 | 0 |
| $V_{cc}$ | 1.6 | 320 | 0 |
| $PLL$ | 30 | 200 | 0 |
| $i_{fd}$ | 120 | 200 | 0 |
| $i_{fq}$ | 120 | 200 | 0 |

TABLE III
TURBINE

| Parameter | Value |
|---|---|
| $R$ | 2.1 ($m$) |
| $\rho$ | 1.21 ($Kg/m^3$) |
| $J_t$ | 5 ($Kg \cdot m^2$) |
| $F_t$ | 0.02 ($N \cdot m \cdot s$) |
| $K_s$ | 0.2 |
| $\alpha$ | 30 |
| $K_v$ | 5 |
| $K_{torsion}$ | 10000 |

TABLE IV
MRAC

| Parameter | Value |
|---|---|
| $k_m$ | 770 |
| $a_m$ | 700 |
| $\gamma_1$ | $10^6$ |
| $\gamma_2$ | $1.5 \cdot 10^6$ |
| $\sigma$ | 10 |

## References


[1] Global wind energy council. url: http://gwec.net/global-figures/graphs/.

[2] Hyong Sik Kim and Dylan Dah-Chuan Lu. Wind energy conversion system from electrical perspective—a survey. *Smart Grid and Renewable Energy*, 1(03):119, 2010.

[3] Md E. Haque, Michael Negnevitsky, and Kashem M. Muttaqi. A novel control strategy for a variable speed wind turbine with a permanent magnet synchronous generator. In *Industry Applications Society Annual Meeting, 2008. IAS'08. IEEE*, pages 1–8. IEEE, 2008.

[4] H. Merabet Boulouiha, A. Allali, A. Tahri, A. Draou, and Mouloud Denai. A simple maximum power point tracking based control strategy applied to a variable speed squirrel cage induction generator. *Journal of Renewable and Sustainable Energy*, 4(5):053124, 2012.

[5] José Luis Domínguez-García, Oriol Gomis-Bellmunt, Lluís Trilla-Romero, and Adrià Junyent-Ferré. Indirect vector control of a squirrel cage induction generator wind turbine. *Computers & Mathematics with Applications*, 64(2):102–114, 2012.

[6] H. Merabet Boulouiha, A. Allali, M Laouer, A. Tahri, Mouloud Denai, and A. Draou. Direct torque control of multilevel svpwm inverter in variable speed scig-based wind energy conversion system. *Renewable Energy*, 80:140–152, 2015.

[7] Shankar Sastry and Marc Bodson. Adaptive control: stability, convergence and robustness. 2011.

[8] Ahmed M. Kassem, Khaled M. Hasaneen, and Ali M. Yousef. Dynamic modeling and robust power control of dfig driven by wind turbine at infinite grid. *International Journal of Electrical Power & Energy Systems*, 44(1):375–382, 2013.

[9] ME. Haque and MF. Rahman. Influence of stator resistance variation on direct torque controlled interior permanent magnet synchronous motor drive performance and its compensation. In *Industry Applications Conference, 2001. Thirty-Sixth IAS Annual Meeting. Conference Record of the 2001 IEEE*, volume 4, pages 2563–2569. IEEE, 2001.

[10] Ciro Attaianese, V. Nardt, Aldo Perfetto, and Giuseppe Tomasso. Vectorial torque control: a novel approach to torque and flux control of induction motor drives. *IEEE Transactions on Industry applications*, 35(6):1399–1405, 1999.

[11] Giuseppe S Buja and Marian P Kazmierkowski. Direct torque control of pwm inverter-fed ac motors-a survey. *IEEE Transactions on industrial electronics*, 51(4):744–757, 2004.

[12] Muhammed Fazlur Rahman, Li Zhong, Md E. Haque, and MA. Rahman. A direct torque-controlled interior permanent-magnet synchronous motor drive without a speed sensor. *IEEE Transactions on Energy Conversion*, 18(1):17–22, 2003.

[13] Jawad Faiz and S. Hossein Mohseni-Zonoozi. A novel technique for estimation and control of stator flux of a salient-pole pmsm in dtc method based on mtpf. *IEEE Transactions on Industrial Electronics*, 50(2):262–271, 2003.

[14] A. R. C. Alves and L. S. Barros. Rastreamento da máxima potência de turbinas eólicas baseadas em máquinas de indução com rotor em gaiola através do controle por escorregamento com fluxo estatórico. *Congresso Brasileiro de Automática (CBA)*, 2018.

[15] Ivo Barbi. *Teoria fundamental do motor de indução*. Editora da UFSC Florianopolis, 1985.

[16] Filipe Emanuel Vieira Taveiros, Luciano Sales Barros, and Camila Mara Vital Barros. Conventional and adaptive strategies applied to dc motor control using microcontroller pic18f4520. In *2018 Simposio Brasileiro de Sistemas Eletricos (SBSE)*. IEEE, 2018.

[17] Thomas G. Habetler and Deepakraj M. Divan. Control strategies for direct torque control using discrete pulse modulation. *IEEE Transactions on Industry Applications*, 27(5):893–901, 1991.

[18] Darlan Alexandria Fernandes, Fabiano Fragoso Costa, and Euzeli Cipriano dos Santos. Digital-scalar pwm approaches applied to four-leg voltage-source inverters. *IEEE Transactions on Industrial Electronics*, 60(5):2022–2030, 2013.

[19] Richard Monopoli. Model reference adaptive control with an augmented error signal. *IEEE Transactions on Automatic Control*, 19(5):474–484, 1974.

[20] Shankar Sastry and Marc Bodson. *Adaptive control: stability, convergence and robustness*. Courier Corporation, 2011.

[21] C. Rohrs, Lena Valavani, Michael Athans, and Gunter Stein. Robustness of continuous-time adaptive control algorithms in the presence of unmodeled dynamics. *IEEE Transactions on Automatic Control*, 30(9):881–889, 1985.

[22] Petros A. Ioannou and Petar V. Kokotovic. Instability analysis and improvement of robustness of adaptive control. *Automatica*, 20(5):583–594, 1984.

[23] A. D. Araújo. Contribuição teoria de controle adaptativo por modelo de referência e estrutura variável: uma abordagem entrada/saıda. *Universidade Federal do Rio de Janeiro, Tese de Doutorado, Rio de Janeiro-RJ*, 1993.